BEST AVAILABLE IMAGES

Defective images within this document are accurate representations of the original documents submitted by the applicant.

Defects in the images may include (but are not limited to):

- BLACK BORDERS
- TEXT CUT OFF AT TOP, BOTTOM OR SIDES
- FADED TEXT
- ILLEGIBLE TEXT
- SKEWED/SLANTED IMAGES
- COLORED PHOTOS
- BLACK OR VERY BLACK AND WHITE DARK PHOTOS
- GRAY SCALE DOCUMENTS

IMAGES ARE BEST AVAILABLE COPY.

As rescanning documents *will not* correct images, please do not report the images to the Image Problem Mailbox.

Oncogene (2003) 22, 2823–2835

www.nature.com/onc

SKIP3, a novel *Drosophila* tribbles ortholog, is overexpressed in human tumors and is regulated by hypoxia

Alex J Bowers[1], Sheila Scully[2] and John F Boylan*[,1]

[1]*Department of Cancer Biology, Amgen Inc., One Amgen Center Drive, Thousand Oaks, CA 91320, USA;* [2]*Department of Pathology, Amgen Inc., One Amgen Center Drive, Thousand Oaks, CA 91320, USA*

Regions of hypoxia are a hallmark of solid tumors. Tumor cells modulate the regulation of specific genes allowing adaptation and survival in the harsh hypoxic environment. We have identified SKIP3, a novel human kinase-like gene, which is overexpressed in multiple human tumors and is regulated by hypoxia. SKIP3 is an ortholog of the *Drosophila* tribbles, rat NIPK, dog C5FW, and human C8FW genes. *Drosophila* tribbles is involved in slowing cell-cycle progression during *Drosophila* development, but little is known regarding the function or tissue distribution of the vertebrate orthologs. We show that the normal tissue expression of SKIP3 is confined to human liver, while multiple primary human lung, colon, and breast tumors express high levels of SKIP3 transcript. Endogenous SKIP3 protein accumulates within 48 h under hypoxic growth conditions in HT-29 and PC-3 cells, with upregulation of the SKIP3 mRNA transcript by 72 h. We identified activating transcription factor 4 (ATF4) as a SKIP3-binding partner using the yeast-two-hybrid assay. Coexpression of SKIP3 and ATF4 showed that SKIP3 is associated with the proteolysis of ATF4, which can be blocked using a proteosome inhibitor. These results indicate that SKIP3 may be an important participant in tumor cell growth.
Oncogene (2003) **22**, 2823–2835. doi:10.1038/sj.onc.1206367

Keywords: SKIP3; ATF4; hypoxia; tumor; gene expression

Introduction

The signaling pathways that drive tumor progression are varied and complex. As the size of a tumor increases, nutrients and oxygen become limiting within the tumor microenvironment. In response to localized nutrient deficiency, increased acidity, and hypoxia, specific signaling pathways are activated in tumor cells to regulate the transcription of genes promoting cell survival (reviewed in Fafournoux *et al.*, 2000; Hockel and Vaupel, 2001; Lal *et al.*, 2001). Some of these transcription factors include the hypoxia-inducible factor 1α (HIF-1α) (reviewed in Semenza, 2000), as well as stress and nutrient deficiency regulated genes, CHOP/GADD153, C/EBPα, C/EBPβ (Fafournoux *et al.*, 2000), the proto-oncogene c-*myc* (Yao *et al.*, 1995), and AP-1 transcription factors c-*jun* (Ausserer *et al.*, 1994) and c-*fos* (Yao *et al.*, 1994). Regulation of these transcription factors occurs at several levels, including upregulation of gene expression by the HIF-1 complex, modulation of protein stability, and selective binding to specific heterodimer partners such as members of the AP-1 and activation transcription factor (ATF)/CREB bZIP transcription factor families. Interestingly, specific members of the bZIP transcription factor family have, to date, not been implicated in tumor progression but are associated with responses to stress pathways, such as low levels of oxygen, the antioxidant response, and general cellular stress. One such bZIP family member is ATF4 (Estes *et al.*, 1995; Gachon *et al.*, 2001; He *et al.*, 2001).

Human ATF4, also known as CREB2, TAXREB67, and C/ATF, is a member of the ATF/CREB (activating transcription factor/cyclic AMP response element binding protein) family of basic region-leucine zipper (bZIP) transcription factors (for review see Hai and Hartman, 2001). ATF4 transactivates the transcription of specific genes through binding to the cAMP response element (CRE) TAGACGTCA (Karpinski *et al.*, 1992). Multiple gene promoters have been identified as being transactivated by ATF4, including *CHOP/GADD153* (Fawcett *et al.*, 1999), interleukin-2 CD28 response element (*CD28RE*) (Butscher *et al.*, 1998), and the adenomatous polyposis coli (APC) tumor suppressor-binding protein *RP1* (Wadle *et al.*, 2001). The transcriptional selectivity of ATF4 is modulated by the formation of heterodimers with multiple C/EBP bZIP proteins including: CHOP/GADD153 (Gachon *et al.*, 2001), C/EBPα (Nishizawa and Nagata, 1992), C/EBPβ, CRP2 (Vallejo *et al.*, 1993), and C/EBPγ (Vinson *et al.*, 1993) as well as AP-1 family members (fos and jun proteins) (Hai and Curran, 1991; Kato *et al.*, 1999). ATF4 also associates with Tax, a human T-cell leukemia virus type I transactivator (Reddy *et al.*, 1997), CREB-binding protein (CBP) (Liang and Hai, 1997), and Zip kinase (Kawai *et al.*, 1998). Additionally, protein stability plays a role in modulating ATF4 function. For example, ATF4 binding with βTrCP, a F-box protein that is part of the E3 ubiquitin ligase complex, leads to ubiquitin-mediated

*Correspondence: JF Boylan;
E-mail: jboylan@amgen.com
Received 3 October 2002; revised 31 December 2002; accepted 6 January 2003

degradation of ATF4 (Lassot *et al.*, 2001). Recently, an ATF4 mouse knockout has shown proliferative defects in the fetal liver, embryonic lens, hair follicles, and overall size of knockout mice, indicating an essential role for ATF4 in normal high-level proliferation in mice (Masuoka and Townes, 2002). Although many ATF4 regulation factors have been identified, the question remains as to why ATF4 participates in multiple stress response and proliferation pathways in normal cells, and yet has not been implicated as being crucial for tumor cell progression.

The *Drosophila* tribbles gene was recently identified as a developmental cell-cycle brake that blocks mitotic progression in the mesoderm during early *Drosophila* gastrulation (Grosshans and Wieschaus, 2000; Mata *et al.*, 2000; Seher and Leptin, 2000). The tribbles protein has a high homology to serine/threonine kinases. Although tribbles contains almost all of the consensus amino acids that correspond to the kinase catalytic core, it is highly divergent through the consensus ATP-binding pocket (Seher and Leptin, 2000). The function of the tribbles protein is to slow cell-cycle progression by inducing the degradation of the CDC25 activators of mitosis orthologs, String and Twine, during *Drosophila* gastrulation (Grosshans and Wieschaus, 2000; Mata *et al.*, 2000).

The mammalian orthologs of *Drosophila* tribbles (dog: C5FW, rat: NIPK, human: C8FW) have been identified in multiple species. In dog thyroid cells, the levels of C5FW protein have been shown to increase upon stimulation with thyrotropin or epidermal growth factor (Wilkin *et al.*, 1997). Expression of neuronal cell death inducible putative kinase (NIPK) is induced when rat neuronal PC6-3 cells are deprived of NGF (Mayumi-Matsuda *et al.*, 1999). A human partial protein, C8FW, was identified as a binding partner of 12-LOX in epidermoid carcinoma A431 cells (Tang *et al.*, 2000). Like tribbles protein, C5FW, NIPK, and C8FW proteins all appear to contain the consensus serine/threonine kinase catalytic core, but lack a consensus ATP-binding pocket. No functional data have been reported for these proteins in mammalian cells, and little is known regarding their regulated expression.

In the present study, a novel human ortholog of *Drosophila* tribbles (SKIP3) was identified and cloned. SKIP3 is highly homologous to tribbles and the vertebrate tribbles orthologs. SKIP3 has a narrow normal human tissue expression, but is overexpressed in multiple human tumors and tumor-derived cell lines. Endogenous levels of SKIP3 mRNA and protein are increased under long-term hypoxic growth conditions, and the SKIP3 protein associates with ATF4 during the proteolysis of both proteins.

Results

Isolation of the SKIP3 cDNA clone

A Hidden Markov Model (Eddy, 1996) was used to search the Celera early access human genomic database to identify novel serine/theronine kinases. To determine whether the identified virtual sequences were differentially expressed in human tumor tissue, a PCR-based assay was designed to screen multiple matched pair normal versus tumor cDNA libraries for potential differential expression patterns. A specific band corresponding to one candidate gene was identified by nonlinear RT–PCR showing overexpression in multiple colon tumor samples when compared to matched normal colon samples (data not shown). This PCR fragment was full-length cloned and sequenced. Sequence homology occurred with multiple ESTs (Genbank Accession #NM021158, Unigene Hs.26802) as well as a recent full-length direct Genbank deposit, identified as SKIP3 (Genbank Accession #AF250311). The full-length mRNA coding sequence is 1077 bases and is predicted to encode a 39.8 kDa protein.

Homology of SKIP3 with known proteins

SKIP3 has very high homology to several previously reported proteins (Figure 1), including rat NIPK (72%), dog C5FW (43%), a recent human full-length C8FW Genbank deposit, SKIP1 (42%), and *Drosophila* tribbles (21%). The highest area of conservation among this family of proteins occurs in the carboxy-terminal half of the proteins. In contrast, the tribbles' amino-terminal protein region is highly variant to the other family members, suggesting that some function of tribbles may vary from its vertebrate counterparts.

Kinase-like features of the SKIP3 protein

Much like the *Drosophila* tribbles, rat NIPK and dog C5FW, SKIP3 has significant sequence homology to several consensus kinase subdomains, but varies to a considerable degree at the predicted ATP-binding subdomains (Figure 2). The region of highest homology includes subdomains VIA–XI of the consensus protein kinase domain (Hanks and Hunter, 1995). Interestingly, SKIP3 is highly variant throughout subdomains I–V, most notably in the ATP-binding pocket, including the glycine-rich loop in subdomain I, the nearly invariant lysine in subdomain II, the glutamic acid in subdomain III, and the valine–methionine motif of subdomain V. The kinase catalytic core of SKIP3 in subdomain VIB is not an exact match with the consensus, RDLKxxN, but instead replaces the asparagine with the basic residue arginine. Also, SKIP3 does not appear to contain either the DFG ATP orientation and transfer motif of subdomain VII nor the serine/threonine phosphorylation activation site of subdomain VIII. Overall SKIP3 contains the classic substrate-binding domains of a protein kinase, but lacks the ATP-binding and kinase-activation domains.

To date, neither SKIP3 nor any of the orthologs have been shown to have kinase activity. To determine SKIP3's ability to act as a kinase, we used SKIP3-myc from transiently transfected U2-0S cell lysates in *in vitro* phosphorylation kinase experiments with α-casein, β-casein, myelin basic protein, or histone H1 as potential substrates of many known serine/threonine kinases. Immunoprecipitated SKIP3-myc was combined

```
   SKIP3    (1) -------------------------MRATPLAAPAGSLSR----------------KKR
    NIPK    (1) -------------------------MRATSLAASADVPCR----------------KKP
    C5FW    (1) ----------------------MNIHRSTPITIARYGRSR----------------NKT
   SKIP1    (1) -------------------------MRVGPVRSAMSGASQPRGPALLFPATRGVPAKRL
Tribbles    (1) MDNSSGQNSRTASSASTSKIVNYSSPVSPGVAAATSSSSSSSSSGMSSSQEDTVLGLFTP
                                          MRATPLAAAA   SR                KK

   SKIP3   (19) LELDDNLDTERPVQKRARSGPQP-RLPPCLLPLSPPTAP------DRATAVATASRLGPY
    NIPK   (19) LEFDDNIDVECPVLKRVRDEPEP-GPTPSLPPAS----------DLSPAVAPATRLGPY
    C5FW   (22) QDFEELSSIRSAEP--SQSFSP--NL---GSPSPPET-P---------NLSHCVSCIGKY
   SKIP1   (35) LDADDAAAVAAKCPRLSECSSPPDYLSPPGSPCSPQPPPAAPGAGGGSGSAPGPSRIADY
Tribbles   (61) KKEFPNAKMLQTIREKLMTPGGACDLLALGIAAEPTDQQPVKLIQQRYLISAQPSHISAA
                LD DDNA V   V KRS S   P  L P G PASP   P        S ASA  SRIG Y

   SKIP3   (72) VLLEPEEGG--------RAYQALHCPTGTEYTCKVYPVQEALAVLEPYARLPPHKHVAR-
    NIPK   (67) ILLEREQGN--------CTYRALHCPTGTEYTCKVYPASEAQAVLAPYARLPTHQHVAR-
    C5FW   (65) LLLEPLEGD--------HVFRAVHLHSGEELVCKVFDISCYQESLAPCFCLSAHSNINQ-
   SKIP1   (95) LLLPLAERE--------HVSRALCIHTGRELRCKVFPIKHYQDKIRPYIQLPSHSNITG-
Tribbles  (121) VAAKTPASYRHLVDLTASNLRCVDIFTGEQFLCRIVNEPLHKVQRAYFQLQQHDEELRRS
                LLLE  EG           YRALHI TG EY CKVFPI  YQ  LAPY  LP H  I R

   SKIP3  (123) ------------------------PTEVLAGTQLLYAFFTRTHGDMHSLVRSRHRIPEPE
    NIPK  (118) ------------------------PTEVLLGSQLLYTFFTKTHGDLHSLVRSRRGIPEPE
    C5FW  (116) ------------------------ITEIILGETKAYVFFERSYGDMHSFVRTCKKLREEE
   SKIP1  (146) ------------------------IVEVILGETKAYVFFEKSFGDMHSYVRSRKRLREEE
Tribbles  (181) TIYGHPLIRPVHDIIPLTKDRTYILIAPVPQERDSTGGVTGVYENLHTYIRHAKRLCETE
                                        ITEVILGE  AY FFTKSHGDMHSYVRSRKRL E E

   SKIP3  (159) AAVLFRQMATALAHCHQHGLVLRDLKLCRFVFADRERKKLVLENLEDSCVLTGPDDSLWD
    NIPK  (154) AAALFRQMASAVAHCHKHGLILRDLKLRRFVFSNCERTKLVLENLEDACVMTGPDDSLWD
    C5FW  (152) AARLFYQIASAVAHCHDGGLVLRDLKLRKFIFKDEERTRVKLESLEDAYILRGDDDSLSD
   SKIP1  (182) AARLFKQIVSAVAHCHQSAIVLGDLKLRKFVFSTEERTQLRLESLEDTHIMKGEDDALSD
Tribbles  (241) ARAIFHQICQTVQVCHRNGIILRDLKLKRFYFIDEARTKLQYESLEGSMILDGEDDTLSD
                AA LFRQIASAVAHCH  GLVLRDLKLRRFVFSDEER  TKL LESLEDA IL GEDDSL

   SKIP3  (219) KHACPAYVGPEILSSRASYSGKAADVWSLGVALFTMLAGHYPFQDSEPVLLFGKIRRGAY
    NIPK  (214) KHACPAYVGPEILSSRPSYSGRAADVWSLGVALFTMLAGRYPFQDSEPALLFGKIRRGTF
    C5FW  (212) KHGCPAYVSPEILNTSGSYSGKAADVWSLGVMLYTMLVGRYPFHDIEPSSLFSKIRRGQF
   SKIP1  (242) KHGCPAYVSPEILNTTGTYSGKAADVWSLGVMLYTLLVGRYPFHDSDPSALFSKIRRGQF
Tribbles  (301) KIGCPLYTAPELLCPQQTYKGKPADMWSLGVILYTMLVGQYPFYEKANCNLITVIRHGNV
                SDKHGCPAYVSPEIL S GSYSGKAADVWSLGVMLYTMLVGRYPFHDSEPS LFSKIRRG

   SKIP3  (279) ALPAGLSAPARCLVRCLLRREPAERLTATGILLHPWLRQDPMPLAPTRSHLWEAAQVVPD
    NIPK  (274) ALPEGLSASARCLIRCLLRREPSERLVALGILLHPWLREDCSQVSPPRSDRREMDQVVPD
    C5FW  (272) NIPETLSPKAKCLIRSILRREPSERLTSQEILDHPWFSTDFSVSNSGYGAKEVSDQLVPD
   SKIP1  (302) CIPEHISPKARCLIRSLLRREPSERLTAPEILLHPWFESVLEPG-YIDSEIGTSDQIVPE
Tribbles  (361) QIPLTLSKSVRWLLLSLLRKDYTERMTASHIFLTPWLREQRPFHMYLPVDVEVAEDWSDA
                QF IPE LS  ARCLIRSLLRREPSERLTA  ILLHPWLR D        SDI  ADQVV

   SKIP3  (339) GLGLDEAREEEGDREVVLYG-----------------------------------------
    NIPK  (334) GPQLEEAEEG----EVGLYG-----------------------------------------
    C5FW  (332) VNMEENLDPFFN-------------------------------------------------
   SKIP1  (361) YQEDSDISSFFC-----------------------------------------------
Tribbles  (421) DAEEDEGTAADAMDDDEEGLCPLGDKHEYEDIGVEPLDYTRSTLQMAQNANGLSTEPEPD
                PD   EEEA E     E  L

   SKIP3  (359) ------
    NIPK  (350) ------
    C5FW  (344) ------
   SKIP1  (373) ------
Tribbles  (479) TDVDMG
```

Figure 1 Sequence comparison of SKIP3 protein with other known proteins having a high degree of similarity. Aligned are potential orthologs of SKIP3, including rat NIPK (Genbank Accession #BAA77582), dog C5FW (Genbank Accession #X99144), and *Drosophila* tribbles (Genbank Accession #AAF26374), as well as a highly related human family member, SKIP1/C8FW (Genbank Accession #AAK58174). Amino acids that are identical between all five proteins are marked in gray, and the consensus sequence is indicated in bold below the alignments

with purified recombinant substrate and [γ-^{32}P]ATP for 30 min. Reactions were analysed by SDS–PAGE. No substrate phosphorylation or autophosphorylation of SKIP3 was observed (data not shown).

Tissue distribution of SKIP3 transcript

Northern blot analysis was performed using full-length SKIP3 as a probe (Figure 3) to determine the tissue distribution of SKIP3 in normal human tissues and tumor-derived cell lines. The full-length 3.5 kb SKIP3 mRNA is most highly expressed in human liver, with very low expression in other tissues. All of the tumor-derived cell lines analysed express SKIP3, with the chronic myelogenous leukemia K-562 having the highest expression. HeLa cell S3, colorectal adenocarcinoma SW480, and melanoma G-361 also expressed high levels of SKIP3 mRNA.

```
subdomain          <          I              ><         II       ><      III      ><
  SKIP3 KD     (1) DRATAVATASRLGPYVLLEPEEGGRAYQALHCPTG-TEYTCKVYPVQEALAVLEPYARLP
   STK2 KD     (1) YCYLRVVGKGSYGEVTLVKHRRDGKQYVIKKLNLR-NASSRERRAAEQEAQLLSQLKHPN
   AMPK KD     (1) YVLGDTLGVGTFGKVKIGEHQLTGHKVAVKILNRQKIRSLDVVGKIKREIQNLKLFRHP-
PKC-alpha KD   (1) FNFLMVLGKGSFGKVMLADRKGTEELYAIKILKKDVVIQDDDVECTMVEKRVLALLDKPP
                   Y PL VLGKGSFGKVMLLEHK TGK YAIKILNK  I SSDDV  I  EIQVLALLKHPP

subdomain            IV       ><          V             ><             VIA
  SKIP3 KD    (60) PHKHVARPTEVLAGTQLLYAFFTRTHGDMHSLVRSRHRIPEPEAAVLFRQMATALAHCHQ
   STK2 KD    (60) IVTYKESWEGGDGLLYIVMGFCEGGDLYRKLKEQKGQLLPENQVVEWFVQIAMALQYLHE
   AMPK KD    (60) HIIKLYQVISTPTDFFMVMEYVSGGELFDYICKHG--RVEEMEARRLFQQILSAVDYCHR
PKC-alpha KD  (61) FLTQLHSCFQTVDRLYFVMEYVNGGDLMYHIQQVG--KFKEPQAVFYAAEISIGLFFLHK
                    ITHLHS   TLA LYIVMEFVSGGDLF HI   G  RIPEPQAV LF QIASAL YLHK

subdomain          ><      VIB      ><        VII        ><      VIII      ><
  SKIP3 KD   (120) HGLVLRDLKLCRFVFADRERKKLVLENLEDSCVLTGPDDSLWDKHACPAYVGPEILSSRA
   STK2 KD   (120) KHILHRDLKTQNVFLTRTNIIKVGDLGIAR--VLENHCDMASTLIGTPYYMSPELFSNKP
   AMPK KD   (118) HMVVHRDLKPENVLLDAHMNAKIADFGLS---NMMSDGEFLRTSCGSPNYTAPEVISGRL
PKC-alpha KD (119) RGIIYRDLKLDNVMLDSEGHIKIADFGMCK--EHMMDGVTTRTFCGTPDYIAPEIIAYQP
                   HGIVHRDLKLDNVLLDA   IKIADFGLAK  VLM DGDSLRT CGTP YIAPEIIS RP

subdomain                IX                        ><        X        ><
  SKIP3 KD   (180) SYSGKAADVWSLGVALFTMLAGHYPFQDSEPVLLFGKIRRGAY-ALPAGLSAPARCLVRC
   STK2 KD   (178) -YN-YKSDVWALGCCVYEMATLKHAFNAKDMNSLVYRIIEGKLPAMPRDYSPELAELIRT
   AMPK KD   (175) -YAGPEVDIWSCGVILYALLCGTLPFDDEHVPTLFKKIRGGVF-YIPEYLNRSVATLLMH
PKC-alpha KD (177) -YG-KSVDWWAYGVLLYEMLAGQPPFDGEDEDELFQSIMEHNV-SYPKSLSKEAVSICKG
                    YAGKAVDVWALGVILYEMLAG HPFDDEDM SLF KIREG V AIPK LSKEAASLIR

subdomain              XI                    >
  SKIP3 KD   (239) LLRREPAERLTATG-----ILLHPWL
   STK2 KD   (236) MLSKRPEERPSVR-----SILRQPYI
   AMPK KD   (233) MLQVDPLKRATIK-----DIREHEWF
PKC-alpha KD (234) LMTKHPAKRLGCGPEGERDVREHAFF
                   LLSKDPAKRLTIK     DIREHPWF
```

Figure 2 Alignment of SKIP3 kinase-like domain with known kinase domains. Alignment of the SKIP3 kinase-like domain with the protein kinase domains of several known functional kinases, PKC-alpha (Genbank Accession #P17252), STK2 (Genbank Accession #NP003148), and AMPK (Genbank Accession #P54646). Protein kinase subdomains are denoted above the alignment. Amino acids that are identical between all four sequences are marked in gray and the consensus sequence is indicated in bold below the alignments. SKIP3 has significant homology to the kinase substrate-binding domains of known kinases (subdomains VIA–XI) but is highly variant within the ATP-binding domains (subdomains I–V)

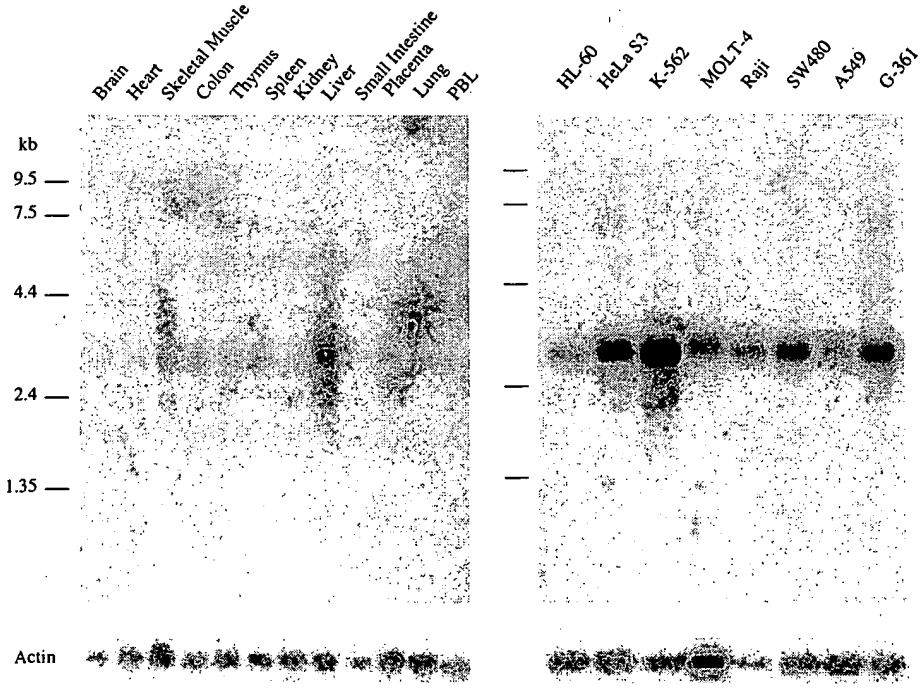

Figure 3 SKIP3 mRNA is highly expressed in normal human liver tissue and multiple human tumor cell lines. Nothern blots hybridized with a radiolabeled probe that corresponds to full-length SKIP3 (nucleotides 1–1077). The Northern blots were exposed to a phosphorimaging screen overnight

Tumor association of SKIP3 transcript

To better define and expand the primary PCR screen, which showed an increase in SKIP3 expression in human colon tumors, human lung and colon tumor tissue samples were analysed for SKIP3 expression in comparison to normal human tissues. Northern blot analysis of SKIP3 mRNA expression in primary human tumor tissue shows that SKIP3 is overexpressed in specific tumor samples including lung adenocarcinoma and colon adenocarcinoma samples, while having a lower relative expression in normal human tissues (Figure 4).

Expanding upon the normal/tumor SKIP3 Northern blot analysis, real-time RT-PCR of SKIP3 across a wide range of tumors from multiple tissues indicates that SKIP3 is overexpressed in specific primary tumor types in comparison with normal tissues (Figure 5). The breast tumors in the analysis had the highest relative overexpression of SKIP3 as well as the broadest expression of SKIP3 of the patient samples tested (Figure 5, upper left panel). These breast tumor types included infiltrating and noninfiltrating ductal carcinomas, lobular carcinoma, and mucinous adenocarcinoma. As determined by nonlinear PCR and Northern blot analysis, real-time RT–PCR of colorectal tumors also showed a broad overexpression of SKIP3 in tumor types including well to moderately differentiated adenocarcinoma, and colon and rectum adenocarcinomas with metastases to the lymph nodes (Figure 5, lower left panel). SKIP3-overexpressing lung tumors included only squamous cell carcinomas and a giant cell carcinoma (Figure 5, upper right panel) although multiple lung adenocarcinomas and keratinizing squamous cell carcinomas were examined. In comparison with breast, colon and lung tumors, uterine and ovarian tumors express SKIP3 at lower relative levels (Figure 5, lower right panel). Within the uterine–ovarian tumor sample group, the highest *SKIP3*-expressing tumor types included uterine moderately to poorly differentiated adenocarcinomas, a uterine malignant mixed Mullerian tumor, and ovarian adenocarcinomas.

To confirm that SKIP3 expression is localized specifically to tumor cells *in situ* hybridization was performed. A full-length SKIP3 probe was used for *in situ* hybridization (ISH) in multiple primary human tumor tissues. Analysis reveals localized SKIP3 expression to specific tumor cells, while surrounding normal tissues show only background hybridization (Figure 6). SKIP3 localizes to specific areas in both lung and colon tumors (Figure 6a, c) with only minimal background hybridization to normal lung and colon tissue (Figure 6b, d). No detectable signal appeared over stromal elements, infiltrating lymphocytes, or adjacent normal

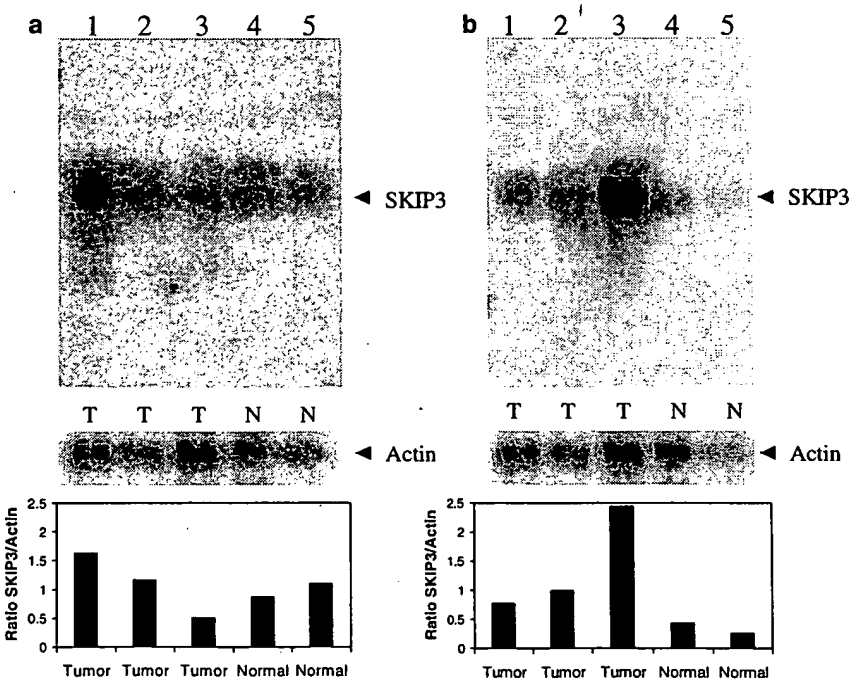

Figure 4 SKIP3 mRNA is upregulated in both primary human lung and colon tumors by Northern blot. (a) Northern blot of human lung tumor and lung tissue mRNA. Lane 1, well-differentiated lung cell adenocarcinoma from a 48-year-old male; lane 2, moderately well differentiated lung cell adenocarcinoma from a 56-year-old male; lane 3, moderately differentiated lung cell carcinoma from a 74-year-old female; lane 4, pooled normal lung tissue from two donors; lane 5, pooled normal lung tissue from five donors. (b) Northern blot of colon tumor mRNA and normal colon from human tissue. Lane 1, moderately differentiated colon cell adenocarcinoma from a 58-year-old male; lane 2, well differentiated colon cell adenocarcinoma from a 63-year-old female; lane 3 well-differentiated colon cell adenocarcinoma from a 35-year-old male; lane 4, pooled normal colon tissue from 10 donors; lane 5, normal lung tissue from one donor. Bar graphs indicate the ratio of SKIP3 levels to levels of actin

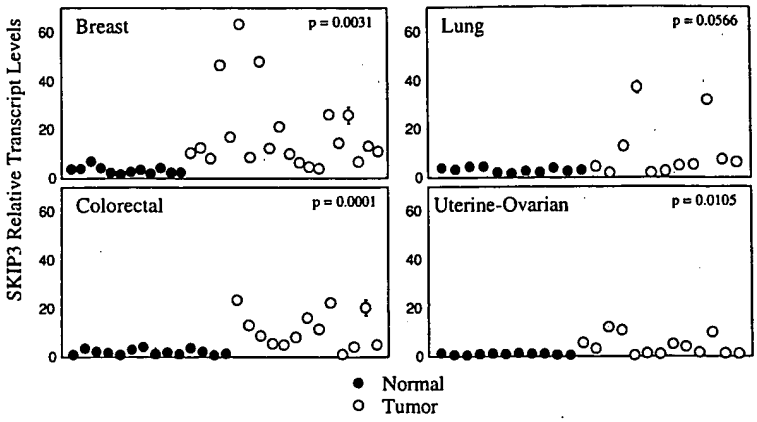

Figure 5 SKIP3 mRNA is overexpressed in multiple primary human tumors as compared to normal tissue. Real-time RT–PCR was performed on total RNA samples from either normal human tissue or primary human tumor tissues. Normal tissue includes samples from both nondisease containing organs as well as normal tumor-adjacent tissue. All values are normalized against 18S rRNA relative transcript levels. *P*-value confidence was calculated using an unpaired comparison *t*-test of the mean difference of normal and tumor SKIP3 transcript levels from each organ; $n=2$

tissues in the tumor samples. These data correlate with the primary tumor/normal Northern and real-time RT–PCR analysis, and suggests that SKIP3 overexpression is not because of highly expressing infiltrating noncancerous cells, but rather is localized to specific cancer cell clusters within each tumor. In addition to primary tumors, SKIP3 localized to tumor cells in metastatic breast carcinoma lesions in the brain (Figure 6e).

To better understand the expression pattern of SKIP3 in primary human tumors, as well as define an experimental system to study SKIP3 expression, ISH was used to analyse SKIP3 expression in human tumor xenografts. HT-29 human colorectal adenocarcinoma cells and PC-3 human prostate adenocarcinoma cells were grown subcutanously in nude mice to a volume of 500 mm^3. Tumors were harvested, sectioned, stained, and probed by ISH for SKIP3 expression (Figure 7a–d). SKIP3 is expressed throughout the HT-29 and PC-3 tumor samples. While SKIP3 is highly expressed in a large percentage of the PC-3 cells (Figure 7c), the expression of SKIP3 is more localized in the HT-29 xenograft (Figure 7a). Although the SKIP3 ISH patterns of both the primary human tumors and the tumor cell xenografts show a specific localized pattern of hybridization, the pattern of SKIP3 expression in the HT-29 xenograft (Figure 7a, yellow arrowheads) appears to be proximal to a region of cell death (Figure 7a, black arrowheads). In the HT-29 xenograft, BrdU-positive cells localized distal from the SKIP3-positive cells (Figure 7b, red arrowheads), indicating that SKIP3 expression does not correlate with cell proliferation. Also for the HT-29 xenograft, we identified the area of cell death (Figure 7a and b, black arrows) as undergoing apoptosis by both the nuclear staining pattern by H&E and the hematoxylin counterstain on the BrdU sections (data not shown). Thus, SKIP3 expression in the HT-29 xenograft localized to a periapoptotic region.

Endogenous regulation of SKIP3 in tumor cell lines

In past studies, HT-29 cells have been shown to undergo apopotosis when exposed to hypoxia (Yao *et al.*, 1995). We hypothesized that the periapoptotic region in the HT-29 xenograft may have contained cells underging a hypoxic response. Expression of SKIP3 was very high in this region and the cells were neither proliferating nor undergoing apoptosis, but instead were located proximal to an apoptotic region. To test this hypothesis, HT-29 and PC-3 cells were cultured under hypoxic conditions for 0, 24, 48, and 72 h to determine if SKIP3 is upregulated at the transcript or protein level under hypoxia. For both HT-29 and PC-3 cells, SKIP3 mRNA expression increases after 72 h under hypoxia (Figure 8a). SKIP3 protein levels begin to increase by 48 h for both HT-29 and PC-3 cells and remain elevated at 72 h (Figure 8b). This is in contrast to SKIP3 protein levels from cells under normoxic conditions that maintain SKIP3 protein at a steady level. Interestingly, many genes that are known to be regulated under hypoxia, such as HIF-1α, VEGF, NDRG1, and carbonic anhydrase (Lal *et al.*, 2001), have been shown to be upregulated at both the transcript and protein levels within 24 h of exposure to hypoxic conditions. The relatively late initiation of expression and protein accumulation of SKIP3 under hypoxia indicates that SKIP3 may be downstream in the hypoxic response pathway relative to the classical hypoxia-activated genes.

Interaction of SKIP3 with ATF4

To begin to understand the functional role of SKIP3 protein in human cells, a yeast-two-hybrid analysis was carried out using full-length SKIP3 fused to a Gal-4 DNA-binding domain as the bait and a cDNA library from normal human liver cells fused to the Gal-4 activation domain as the prey. A human liver cDNA

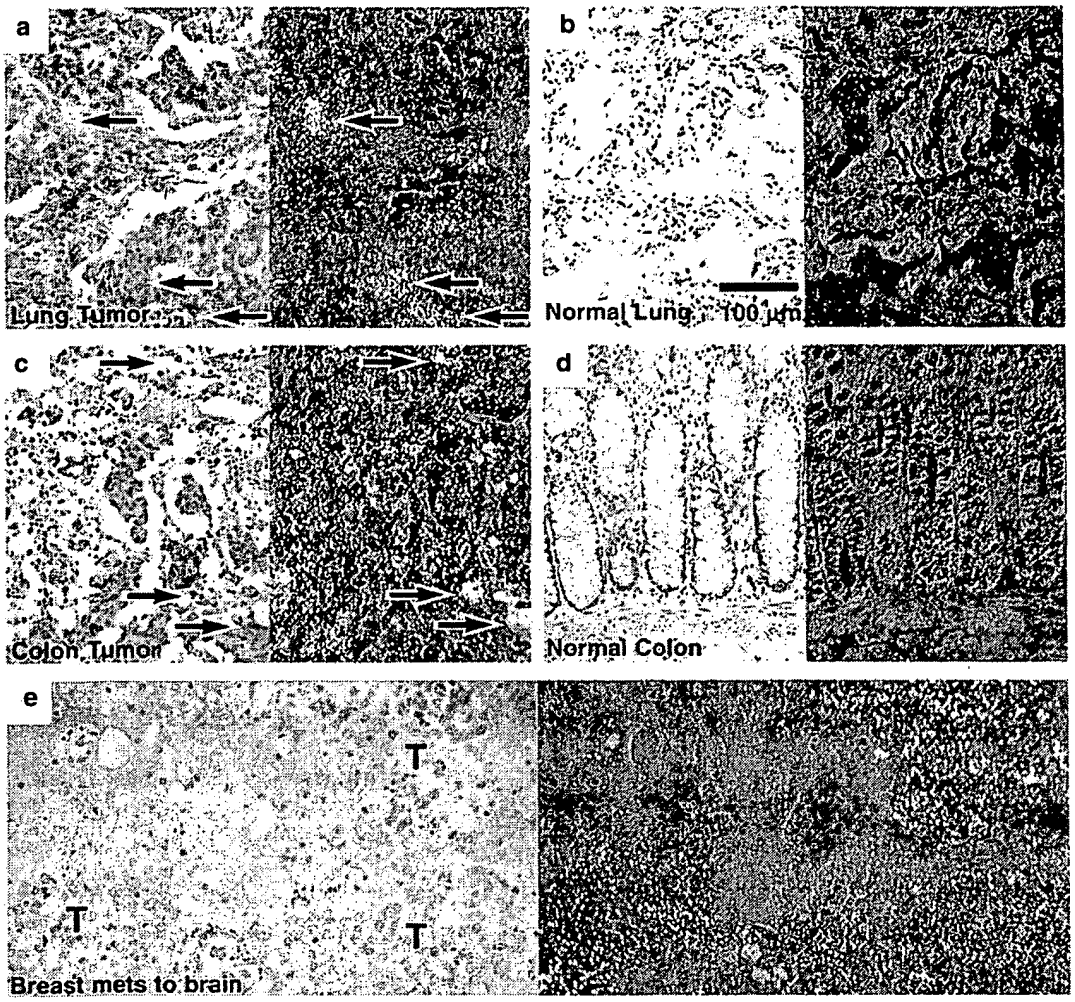

Figure 6 ISH detects SKIP3 mRNA in human tumors. SKIP3 mRNA is clearly present over tumor cells in a human lung adenocarcinoma (a) and a poorly differentiated human colon adenocarcinoma (c) but not detectable in normal human lung (b) or colon (d) or in stromal elements and infiltrating lymphocytes within the tumor sections. Arrows indicate tumor cells expressing high levels of SKIP3. In a section of a human breast tumor metastatsis to brain (e), SKIP3 ISH signal is present over tumor areas (T) but not over adjacent areas of nonmalignant brain tissue. For all panels, a brightfield H&E stain is on the left and SKIP3 ISH photographed under darkfield illumination is on the right

library was chosen because of the increased SKIP3 expression in normal human liver seen by Northern blot analysis. A total of 200 positive colonies were screened and the library inserts were sequenced. In total, 60% of the positive colonies contained the full-length coding sequence for basic region-leucine zipper transcription factor ATF4/CREB2 (Genbank Accession NM001675), 30% contained a 5′ truncated ATF5/ATFx (Genbank Accession NM012068) that was missing the first 171 nucleotides of the gene but was otherwise inframe and intact, and 10% contained cryptic sequence.

Transient overexpression and coimmunopreciptiation of SKIP3 and ATF4 in U2-0S cells was performed to confirm the yeast-two-hybrid result and investigate the interaction of SKIP3 and ATF4 (Figure 9). Cells were transfected with SKIP3 fused to the myc epitope (SKIP3-myc), ATF4 fused to the HA epitope (ATF4-HA), or SKIP3-myc and ATF4-HA in combination. Transfected cells were treated with the proteasome inhibitor MG132 as indicated. Transfection efficiency was 30–35% as monitored by cotransfection of a GFP encoding vector (data not shown). Cotransfection of SKIP3 with ATF4 resulted in the reduced expression of both proteins by Western blot (Figure 9a, lane 7). Treatment with the proteasome inhibitor MG132 restored the levels of both proteins in the cotransfection, consistent with the idea that SKIP3 and ATF4 reduction was a result of proteolysis (Figure 9a, lane 8). This result was also replicated with a second proteasome inhibitor, lactacystin (data not shown). Thus, SKIP3 and ATF4 transfected alone are not targeted for degradation, but upon cotransfection the levels of both the proteins are reduced.

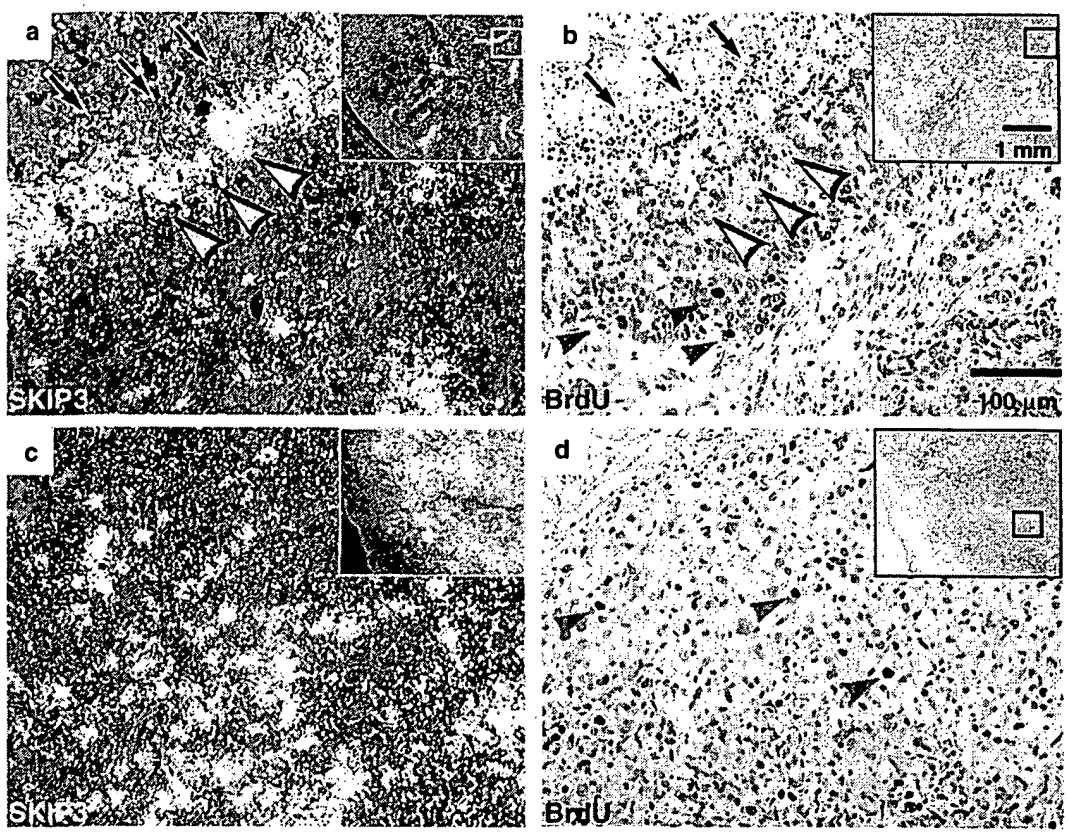

Figure 7 ISH detects SKIP3 mRNA in human tumor xenografts grown subcutaneously in nude mice. Both HT-29 colon carcinoma (**a** and **b**) and PC-3 prostate carcinoma (**c** and **d**) xenografts express SKIP3 mRNA. Low-magnification insets show the distribution of signal in the tumor mass with the boxed areas shown at higher magnification in the large panels. SKIP3 expression does not correlate with proliferation as measured by BrdU labeling (dark brown stained nuclei indicated by red arrowheads in **b** and **d**). In the HT-29 xenograft, SKIP3 ISH signal (yellow arrowheads) is present over cells proximal to an area of apoptosis (black arrows). In the PC3 xenograft, SKIP3 is expressed throughout the tumor. Panels a and c are SKIP3 ISH photographed under darkfield illumination. Panels b and d are adjacent sections immunostained for BrdU, low magnification insets are H&E stained

Although we observed a decrease in the levels of SKIP3-myc and ATF4-HA proteins when cotransfected (Figure 9a, lane 7 and Figure 9b, upper two panels), upon coimmunoprecipitation, the anti-HA antibody was able to coprecipitate SKIP3-myc (Figure 9b, lower panel). The reverse coimmunoprecipitation of ATF4-HA using anti-myc as the precipitating antibody and Western blotting with anti-HA was attempted; however, nonspecific binding of the anti-HA antibody to the heavy chain of the precipitating anti-myc antibody obscured any potential ATF4 banding pattern by Western blot (data not shown). Thus, despite the decreased protein levels of SKIP3 and ATF4 in the cotransfection, we were able to confirm the yeast-two-hybrid results and demonstrate that SKIP3 and ATF4 interact under transient transfection conditions in U2-0S cells. This interaction appears to change the protein stability of both SKIP3 and ATF4.

Interestingly, *Drosophila* tribbles has been shown to interact with and activate the proteolysis of a *Drosophila* ATF-C/EBP basic region-leucine zipper transcription factor family member, slbo, using similar overexpression and coimmunoprecipitation studies (Rorth *et al.*, 2000). It appears that a SKIP3-bZIP transcription factor interaction has been conserved in *Drosophila* and humans in both binding ability and activation of proteolysis. This is consistent with the importance of protein stability in the regulation of the SKIP3 family of kinase-like proteins.

Discussion

SKIP3 is a new member of the kinase-like *Drosophila* tribbles family. These proteins encode the consensus sequence for a serine/threonine catalytic core, but do not contain a classical ATP-binding pocket nor have they been shown to possess enzymatic activity. Despite the lack of tribbles kinase activity, in past studies, the invariant lysine 266 of the putative kinase catalytic core of tribbles was mutated to an arginine to define if these residues contributed to nonkinase tribbles activity. This mutation in tribbles did not change its functional activity (Grosshans and Wieschaus, 2000), indicating that the putative serine/threonine kinase catalytic core is

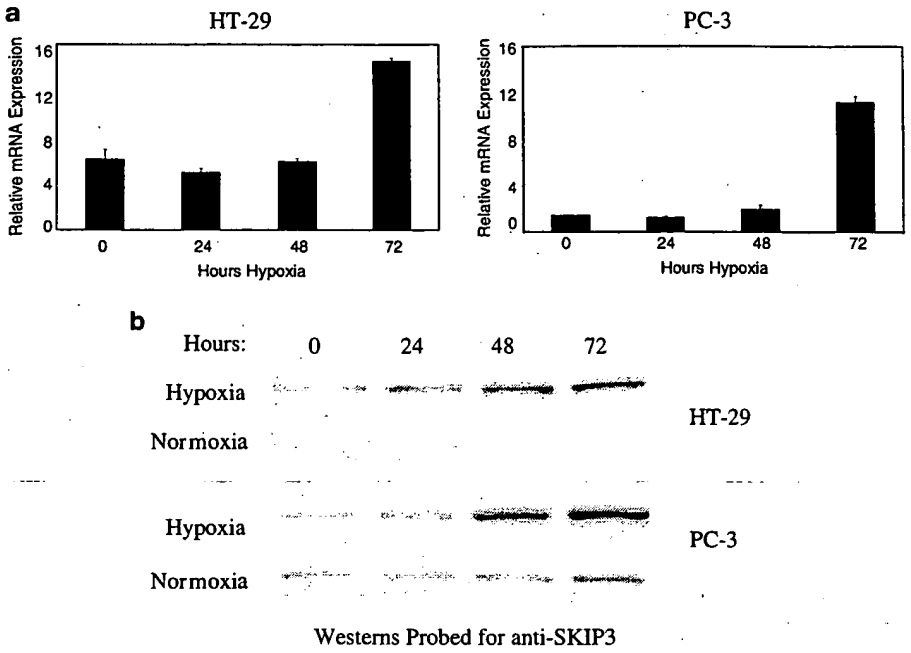

Figure 8 Endogenous SKIP3 mRNA transcript and protein expression accumulates over time under hypoxic growth conditions. HT-29 or PC-3 cells were grown under hypoxia or normoxia for 0, 24, 48 and 72 h. (a) TaqMan PCR analysis of SKIP3 mRNA expression. All values are normalized against 18S rRNA levels, $n=3$. (b) Westerns probed with anti-SKIP3 polyclonal antibody from direct cell lysates

not required for tribbles function. Similarly, in this study, SKIP3 was shown to lack kinase activity using several traditional serine/threonine kinase substrates. Thus, SKIP3 is most likely not a kinase, or does not function as what is currently thought of as a classical kinase.

Without SKIP3 kinase activity, the question remains as to the function of SKIP3 in human cells. To begin to address this question, we examined the data that exist for the SKIP3 orthologs. Very little is known about the function of SKIP3 orthologs in vertebrate cells. Rat NIPK expression is upregulated under NGF depletion stress conditions in rat neuronal cells (Mayumi-Matsuda *et al*., 1999). C8FW, originally identified as a partial protein, was recently deposited in Genbank as a full-length clone named SKIP1. C8FW/SKIP1 was shown to bind to the arachidonic acid metabolizing enzyme 12-LOX. Interestingly, 12-LOX has been shown to be overexpressed in human cancer tissue (Tang *et al*., 2000). With SKIP3 and C8FW/SKIP1 having such a high degree of homology, and SKIP3 showing a broad tumor expression pattern, it would be interesting to know the tumor expression profile of C8FW/SKIP1, as well as whether C8FW/SKIP1 binds to ATF4 or other ATF family members.

With only limited functional data for SKIP3, and the vertebrate orthologs of SKIP3, we focused on the data that exist for *Drosophila* tribbles to help infer function for SKIP3. Tribbles has been termed a cell-cycle brake, and has been shown to be essential for blocking mitosis in the *Drosophila* mesoderm during early gastrulation (Seher and Leptin, 2000). Tribbles initiates a delay in ventral furrow formation when overexpressed in the *Drosophila* zygote, inhibits mitosis following microinjection of tribbles mRNA in cleavage stage *Drosophila* embryos (Grosshans and Wieschaus, 2000), and slows progression through G2 when overexpressed in *Drosophila* imaginal disc cells (Mata *et al*., 2000). This G2 slowing can be reversed when the *Drosophila* CDC25 ortholog, string, is coexpressed with tribbles. Interestingly, tribbles is able to bind to string and activate its proteolysis (Mata *et al*., 2000). Tribbles has also been shown to bind slbo, a C/EBP bZIP *Drosophila* transcription factor, and activate slbo proteolysis (Rorth *et al*., 2000) through ubiquitination. Thus, the data show that tribbles is able to slow the progression of the cell cycle during development in *Drosophila*. We can infer that SKIP3 may also have the ability to slow the progression of proliferating cells.

In our study, the *Drosophila* tribbles–slbo binding and proteolysis data has been replicated using the mammalian ortholog, SKIP3. Yeast-two-hybrid analysis from a human liver library showed that SKIP3 binds to the bZIP transcription factor ATF4. Interestingly, as in the *Drosophila* studies, treatment with a proteosome inhibitor blocks the degradation of ATF4, consistent with the idea that the reduction in SKIP3 and ATF4 proteins is through proteolysis. These data directly correlate with the binding and proteolysis of *Drosophila* tribbles and slbo and indicate that the binding of tribbles family

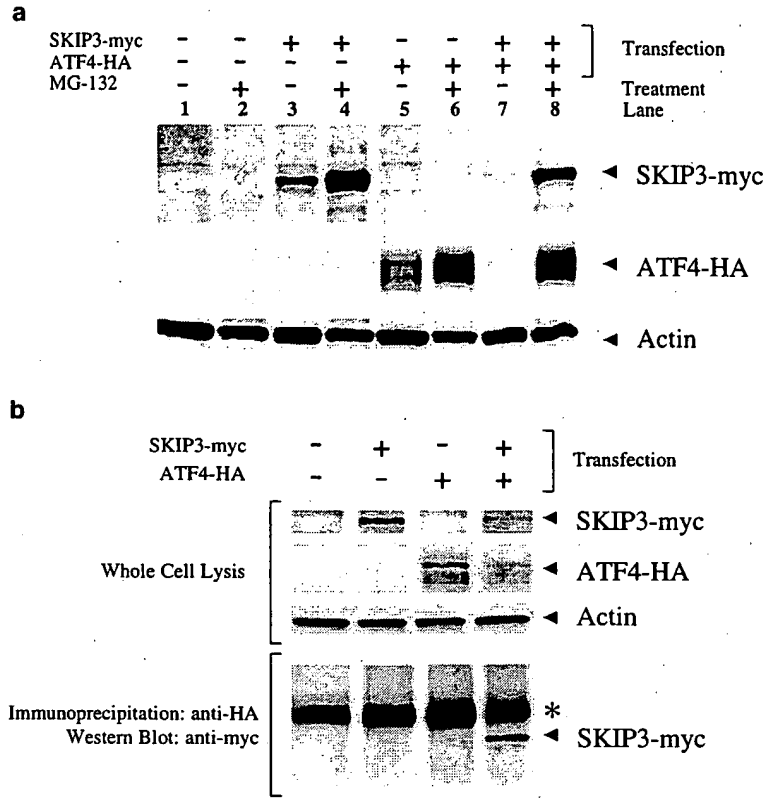

Figure 9 SKIP3 participates in the proteolysis of ATF4 and coimmunoprecipitates with ATF4. (**a**) Western blots of whole-cell lysates of U2-0S cells transfected with expression vectors encoding SKIP3-myc, ATF4-HA and treated with the proteasome inhibitor MG-132 as indicated. SKIP3-myc was detected with anti-SKIP3 antibody, ATF4-HA was detected with anti-HA antibody. (**b**) Whole-cell lysates (upper three panels) and immunoprecipitation of ATF4-HA with anti-HA antibody (lower panel) from U2-0S cells transfected with expression vectors encoding SKIP3-myc and/or ATF4-HA, as indicated. SKIP3-myc was detected with anti-myc antibody. An *indicates crossreactivity with the heavy chain of the immunoprecipitation antibody

members to bZIP transcription factors is a response pathway that has been conserved from *Drosophila* to vertebrates. The question remains as to the participation of ubiquitin in this process, although one can infer from the tribbles–slbo data that the SKIP3–ATF4 degradation may be ubiquitin mediated. An ATF4 *Drosophila* ortholog has been identified as cryptocephal (crc) (Hewes *et al*., 2000). It would be interesting to know whether crc binds to tribbles in a functional manner in *Drosophila* similar to what has been observed here with SKIP3 binding to ATF4 in mammalian cells. Previously, ATF4 has been shown to be activated under stress conditions (Novoa *et al*., 2001), and is able to enhance the transcription of multiple cellular stress response proteins. ATF4 has also been shown to be degraded by the E3 ubiquitin ligase SCF-βTrCP in HeLa cells, although the reasons behind the degradation have yet to be identified (Lassot *et al*., 2001). We show here that SKIP3 is associated with the proteolysis of ATF4. It would be interesting to know if SKIP3 is also a necessary participant in the proteolysis of ATF4 by SCF-βTrCP.

It is interesting to note that no mammalian orthologs of *Drosophila* CDC25 string and twine were found by yeast-two-hybrid analysis of SKIP3. This may be because of the human liver cDNA bait library that was chosen for the SKIP3 yeast-two-hybrid. Normal human tissue expression analysis had shown that SKIP3 was highly expressed in human liver tissue, and so a liver cDNA bait library was chosen for the yeast-two-hybrid. In the future, analysis of SKIP3 in a yeast-two-hybrid using a cDNA library derived from tumor tissue or tissue in which stress pathways are induced would be of value. SKIP3 and ATF4 may interact differently under disease conditions or stress conditions, and additional functional binding partners may interact with SKIP3, including CDC25, or other bZIP family members.

ISH analysis of SKIP3 determined that SKIP3 expression is localized throughout both primary human tumors and human tumor xenografts. The PC-3 xenograft had broad pockets of SKIP3 RNA expression, while the HT-29 xenograft showed more localized and defined regions of SKIP3 expression. In the HT-29 xenograft, SKIP3 localized to periapoptotic regions, in which the cells were neither proliferating nor undergoing apoptosis. We hypothesize that SKIP3 may be functioning in a response to hypoxia since this region was proximal to a region of cells undergoing apoptosis and

HT-29 xenografts are known to have areas of hypoxia that undergo apoptosis. To test this hypothesis, we grew HT-29 and PC-3 cells in tissue culture under hypoxia and analysed the lysates for both SKIP3 mRNA and protein expression. SKIP3 protein accumulated under hypoxia, but only after 48 h. SKIP3 mRNA transcript was upregulated by 72 h. This indicates that there is a feedback response of SKIP3 protein accumulation activating a higher expression of SKIP3 transcript. Many known hypoxia-induced proteins have been characterized as being upregulated within 24 h of exposure to hypoxia. Therefore, because of its relatively late increase in expression, SKIP3 may be part of a later response to hypoxia, and may be under the regulation of one of the known early response hypoxic transcription factors, such as HIF1. This idea is supported by the broad expression of SKIP3 as seen in the PC-3 xenografts. It has been shown previously that the PC-3 cells have a high level of HIF1α expression (Saramaki *et al*., 2001). Combining these data with our observations of late-stage hypoxic expression of SKIP3 and high levels of SKIP3 expression in PC-3 xenografts, we suggest that SKIP3 functions downstream of the HIF1 transcriptional activation pathway.

In this study, the questions of why tumor cells upregulate SKIP3 and why dual expression of SKIP3 and ATF4 activates the reduction of both proteins, remain. ATF4 has not been implicated in tumor progression, but yet is known to participate in both stress response and proliferation pathways (Hai and Hartman, 2001; Masuoka and Townes, 2002). If SKIP3 functions in a similar manner to *Drosophila* tribbles, it is possible that tumor cells activate the expression of SKIP3 to slow down cell-cycle progression and reduce the action of stress-induced genes, namely through the reduction of ATF4 protein levels. The tumor cells may be activating this pathway to provide the cell time to cope with hypoxic stress. Our hypothesis is that SKIP3 is upregulated in hypoxic tumor cells to decrease the ATF4 levels, thereby downregulating the stress signal, slowing the cell cycle and giving the tumor cell time to adapt to its harsh environment. This hypothesis is bolstered by the fact that SKIP3 is upregulated relatively late in cells exposed to hypoxic conditions. Early in hypoxia, tumor cells upregulate transcription factors such as HIF-1α to begin production of proteins that will allow the tumor cell to survive. This includes the establishment of a blood supply through the HIF-1α-induced expression of VEGF. As the hypoxic response progresses, the tumor cell must induce factors that will keep it from undergoing apoptosis. One of these factors may be SKIP3.

Materials and methods

SKIP3 cloning

A Hidden Markov Model (Eddy, 1996) built against known serine/threonine catalytic cores was used to query the Celera human genomic database. A putative kinase-like fragment was identified and PCR primers were designed; 5′-TGGTGCT GGAGAACC TGGAGG-3′ and 5′-CGAGTCCTGGAA GGGGTAGTG-3′. These primers were used to screen the human lung Rapid-Screen Arrayed cDNA Library Panel (Origene Technologies, Rockville, MD, USA) for the full-length SKIP3 cDNA. The positive full-length SKIP3 clone was three-way sequence walked for confirmation. The sequence obtained has a 99% sequence identity to a direct Genbank submission, SKIP3, (Genbank accession #AF250311), and was used in all subsequent experiments and alignments. Our SKIP3 amino-acid sequence differs slightly from the SKIP3 Genbank direct submission, namely, the valine at position 114 is replaced by a leucine in our sequence as well as the aspartic acid at position 194 is instead a glutamic acid. Also, the glutamic acid at postion 196 and the lysine at position 197 in the Genbank SKIP3 direct submission are nonexistent in our SKIP3 sequence.

Northern blots

The human multiple tissue Northern blot and cancer cell line multiple tissue Northern blot (Clontech, Palo Alto, CA, USA) as well as the lung and colon human single-tumor mRNA multi-sample Northern blots (Biochain, San Leandro, CA, USA). SKIP3-radiolabled hybridization probe was generated using full-length SKIP3 cDNA (nucleotides 1–1077) with High Prime cDNA labeling kit (Roche Diagnostics, Indianapolis IN, USA) according to the maunfacturer's instructions. Blots were prehybridized with 10 ml UltraHyb (Ambion, Austin, TX, USA) at 42°C for 3 h, hybridized with radiolabeled SKIP3 cDNA for 18 h, washed for 15 min four times at room temperature with wash buffer 1 (2 × SSC, 0.05% SDS) followed by two washes at 50°C with wash buffer 2 (0.1 × SSC, 0.1% SDS). The blots were exposed to a phosphorimaging screen for 24 h and visualized on a phosphorimager (Molecular Dynamics) at 100 μm resolution.

Real-time RT–PCR

Total RNA samples from normal human and primary human tumor tissues were purchased directly from suppliers; Biochain (San Leandro, CA, USA), Clontech (Palo Alto, CA, USA), and Ambion (Austin, TX, USA). Total RNA samples were adjusted to 5 ng/μl. Real-time PCR was carried out using SKIP3 primers 5′-CGGCTACCACATCCAAGGA-3′, 5′-GCTGGAATTACCGCGGCT-3′, and a probe of 5′-ETG CTGGCACCAGACTTGCCCTCX-3′, where E represents 6-FAM and X represents TAMRA. For normalization, the primers to 18S rRNA were 5′-AATCCTTGAAGGAAATGA-CATTGAG-3′, 5′-TCCTTGTTTTTAACTGTTGTGGCTT-3′ and a probe of 5′-ETTGTTTCAAATTCAGCGGCTTT-GATTCAGX-3′, where E represents 6-FAM and X represents TAMRA. Real-time RT–PCR was performed in a 50 μl reaction with 25 ng sample total RNA using the one-step RT–PCR master mix reagent (Applied Biosystems, Foster City, CA, USA) on an ABI Prism 7700 sequence detector (Perkin-Elmer, Wellesley, MA, USA). Samples were run in duplicate and normalized to the relative transcript level of 18S rRNA. *P*-value confidence was calculated using an unpaired comparison *t*-test of the mean difference of the 18S rRNA normalized normal and tumor SKIP3 transcript levels from each organ.

Xenografts and ISH

HT-29 and PC-3 human tumor cells were grown as xenografts in nu/nu mice by injection of 5×10^6 cells into the right flank. At 1 h being prior to killed, each animal received an

intravenous injection of bromodeoxyuridine (BrdU) (Aldrich Chemical Co., Milwaukee, WI, USA), 50 mg/kg body weight. Tumors grew to about 500 mm^3 and were harvested and fixed for histological and *in situ* analysis. A γ-^{33}P-labeled antisense RNA probe corresponding to full-length SKIP3 (nucleotides 1–1077) was hybridized to 5 μm thick sections of paraffin-embedded tissue followed by RNase digestion and a high stringency wash as previously described (Wilcox, 1993). Signal was detected by emulsion autoradiography, then sections were counterstained with hematoxylin and eosin (H&E) and photographed using darkfield illumination.

Assessment of proliferating cells using anti-BrdU

Paraffin sections adjacent to those used for ISH were incubated with a rat anti-BrdU antibody (Harlan Sera Lab) followed by biotinylated rabbit anti-rat secondary antibody (DAKO Corp. Carpenteria, CA, USA), then peroxidase-linked avidin–biotin complex (Vector Labs, Burlingame, CA, USA) detected with diaminobenzidine/H_2O_2. Sections were counterstained with hematoxylin.

Tissue culture and hypoxic treatment

Human HT-29 colorectal adenocarcinoma cells (ATCC# HTB-38), PC-3 prostate adenocarcinoma cells (ATCC# CRL-1435), and U-2 0S osteosarcoma cells (ATCC HTB-96) were obtained from American Type Culture Collection (Rockville, MD, USA). All cell lines were propagated as per the manufacturer's instructions unless otherwise noted. Hypoxic growth was induced in a Bactron Anaerobic Chamber (Sheldon Manufacturing Inc.) under 0.5% O_2, 5% CO_2 and 94.5% N_2 at 37°C. The MG-132 proteasome inhibitor (Calbiochem, San Diego CA, USA) was dosed for 18 h at 10 μM.

SKIP3 antibody generation

Polyclonal antibodies were generated by immunizing rabbits with synthetic peptides (KLH coupled) corresponding to three different regions within SKIP3, amino acids 20–43, 69–93 and 326–349. Antibody purification was performed using Immunopure Protein A/G (Pierce, Rockford, IL, USA). The three purified antibodies were used to probe Western blots in an equal-volume ratio.

Plasmids

The SKIP3 myc-tagged mammalian expression vector was generated by first PCR modification of full-length SKIP3 with primers 5′-GCCCTTACGACCATGGGAGATGCGAGCC-3′ and 5′-ATCTGCGGCCGCGCCATACAGAACCACT TC-3′ to insert *Nco*I and *Not*I restriction sites into the 5′ and 3′ ends of the full-length SKIP3 cDNA, respectively. T/A cloning (Invitrogen, Carlsbad CA, USA) was used to aneal and amplify the fragment as per the manufacturer's directions. The modified product was digested with *Nco*I and *Not*I and subcloned into pCMV-myc-cyto (Invitrogen, Carlsbad CA, USA). For the yeast-two-hybrid pGBKT7-SKIP3 GAL4 DNA-binding domain fusion, SKIP3 was PCR modified from pCMV-SKIP3-myc with the primers 5′-TGGCCACCATGG-CATATGCGAGCCACCCCT-3′ and 5′- TTTTGGATCT GGTCGACCGCCATACAGAAC-3′ to insert *Nde*I and *Sal*I sites into the 5′ and 3′ ends of the full-length SKIP3 cDNA, respectively. T/A cloning (Invitrogen, Carlsbad CA, USA) was then used to aneal and amplify the fragment as per the manufacturer's directions. The modified product was then digested with *Nde*I and *Sal*I and subcloned into pGBKT7 (Clontech, Palo Alto, CA, USA). pCMV-HA-ATF4 was generated by first full-length PCR cloning ATF4 from the human liver Marathon cDNA library (Clontech, Palo Alto, CA, USA) using the primers 5′-TTCGAATTAAGCA-CATTCCTC-3′ and 5′-ATGACCGAAATGAGCTTCCT-3′. The PCR fragement was T/A cloned and amplified using the primers 5′-GCCCTTTTCGTCGACAGCACATTCCTC-GAT-3′ and 5′-GAATTCGGCGGCCGCCTAGGG-GACCCTTTT-3′ to insert *Sal*I and *Not*I restriction sites into the 5′ and 3′ ends of the ATF4 cDNA, respectively. The PCR fragement was T/A cloned and amplified, then digested with *Sal*I and *Not*I and subcloned into pCMV-HA (Clontech, Palo Alto, CA, USA).

Two-hybrid screen

Saccharomyces cerevisiae AH109 was transformed with pGBKT7-SKIP3 and mated to MatchMaker Y187 pretransformed liver cDNA library (Clontech, Palo Alto, CA, USA). X-α-gal-positive transformants were selected according to the manufacturer's instructions.

Transient transfections

For all transient transfections, 2×10^5 cells were plated per well of a six-well plate and grown for 24 h. A 2.25 μg weight of the indicated plasmid DNA was transfected along with 0.25 μg Green Lantern GFP DNA (Invitrogen, Carlsbad CA, USA), to assess transfection efficiency, for 24 h with FuGENE transfection reagent (Roche Diagnostics, Indianapolis, IN, USA) according to the manufacturer's instructions. Cells were grown for an additional 24 h and harvested.

Immnoprecipitations and Western blotting

Cells were harvested by washing one time with PBS and incubating with TG buffer + 1% IGEPAL (TG buffer: 1% Triton X-100, 10% glycerol, 20 mM HEPES, pH 7.2, 100 mM NaCl, 10 mM NaF, 10 mM Na_3VO_4, 1 tablet Complete Protease Inhibitor (Roche Diagnostics, Indianapolis IN, USA) per 25 ml and Pefabloc (Roche Diagnostics, Indianapolis, IN, USA)) for 10 min at 4°C. Cells were scraped and cell debris was pelleted at 3000 *g* for 5 min. The supernatant was incubated with 6 μg of the indicated antibody for 1 h at 4°C, 50 μl of ImmunoPure Protein A/G (Pierce, Rockford IL, USA) was added and incubated for 30 min at 4°C. The reaction was washed three times in TG buffer + 1 M NaCl and one time in TG buffer alone. The precipitations were heated at 100°C for 5 min with 100 μl sample loading buffer (125 mM Tris HCl, pH 6.8, 5% SDS, 20% glycerol, 12% bromophenol blue, 5% 2-mercaptoethanol), centrifuged and loaded directly onto 12% SDS–PAGE gels to resolve total protein. Proteins were transferred to Protran nitrocellulose (Schleicher and Schuell) blocked for 1 h in 5% powdered milk + 1 × PBS + 0.2% Tween. A 6 μg weight of the indicated antibody was incubated with the blot overnight at 4°C. The blots were developed using the Vectastain kit (Vector Laboratories, Burlingame, CA, USA) as per the manufacturer's instructions and the Renaissance Western blot chemiluminescence reagent kit (NEN, Boston, MA, USA).

Acknowledgements
We thank Marc Payton for providing the isolated total RNA from primary tumor samples for the TaqMan RT–PCR analysis and Tammy L Bush for providing the xenograft tumor material.

References

Ausserer WA, Bourrat-Floeck B, Green CJ, Laderoute KR and Sutherland RM. (1994). *Mol. Cell. Biol.*, **14**, 5032–5042.
Butscher WG, Powers C, Olive M, Vinson C and Gardner K. (1998). *J. Biol. Chem.*, **273**, 552–560.
Eddy SR. (1996). *Curr. Opin. Struct. Biol.*, **6**, 361–365.
Estes SD, Stoler DL and Anderson GR. (1995). *Exp. Cell Res.*, **220**, 47–54.
Fafournoux P, Bruhat A and Jousse C. (2000). *Biochem. J.*, **351**, 1–12.
Fawcett TW, Martindale JL, Guyton KZ, Hai T and Holbrook NJ. (1999). *Biochem. J.*, **339**, 135–141.
Gachon F, Gaudray G, Thebault S, Basbous J, Koffi JA, Devaux C and Mesnard J. (2001). *FEBS Lett.*, **502**, 57–62.
Grosshans J and Wieschaus E. (2000). *Cell*, **101**, 523–531.
Hai T and Curran T. (1991). *Proc. Nat. Acad. Sci. USA*, **88**, 3720–3724.
Hai T and Hartman MG. (2001). *Gene*, **273**, 1–11.
Hanks SK and Hunter T. (1995). *FASEB J.*, **9**, 576–596.
He CH, Gong P, Hu B, Stewart D, Choi ME, Choi AM and Alam J. (2001). *J. Biol. Chem.*, **276**, 20858–20865.
Hewes RS, Schaefer AM and Taghert PH. (2000). *Genetics*, **155**, 1711–1723.
Hockel M and Vaupel P. (2001). *J. Nat. Cancer Inst.*, **93**, 266–276.
Karpinski BA, Morle GD, Huggenvik J, Uhler MD and Leiden JM. (1992). *Proc. Nat. Acad. Sci. USA*, **89**, 4820–4824.
Kato Y, Koike Y, Tomizawa K, Ogawa S, Hosaka K, Tanaka S and Kato T. (1999). *Mol. Cell. Endocrinol.*, **154**, 151–159.
Kawai T, Matsumoto M, Takeda K, Sanjo H and Akira S. (1998). *Mol. Cell. Biol.*, **18**, 1642–1651.
Lal A, Peters H, St Croix B, Haroon ZA, Dewhirst MW, Strausberg RL, Kaanders JH, van der Kogel AJ and Riggins GJ. (2001). *J. Nat. Cancer Inst.*, **93**, 1337–1343.
Lassot I, Segeral E, Berlioz-Torrent C, Durand H, Groussin L, Hai T, Benarous R and Margottin-Goguet F. (2001). *Mol. Cell. Biol.*, **21**, 2192–2202.
Liang G and Hai T. (1997). *J. Biol. Chem.*, **272**, 24088–24095.
Masuoka HC and Townes TM. (2002). *Blood*, **99**, 736–745.
Mata J, Curado S, Ephrussi A and Rorth P. (2000). *Cell*, **101**, 511–522.
Mayumi-Matsuda K, Kojima S, Suzuki H and Sakata T. (1999). *Biochem. Biophys. Res. Commun.*, **258**, 260–264.
Nishizawa M and Nagata S. (1992). *FEBS Lett.*, **299**, 36–38.
Novoa I, Zeng H, Harding HP and Ron D. (2001). *J. Cell Biol.*, **153**, 1011–1022.
Reddy TR, Tang H, Li X and Wong-Staal F. (1997). *Oncogene*, **14**, 2785–2792.
Rorth P, Szabo K and Texido G. (2000). *Mol. Cell*, **6**, 23–30.
Saramaki OR, Savinainen KJ, Nupponen NN, Bratt O and Visakorpi T. (2001). *Cancer Genet. Cytogenet.*, **128**, 31–34.
Seher TC and Leptin M. (2000). *Curr. Biol.*, **10**, 623–629.
Semenza GL. (2000). *Genes and Dev.*, **14**, 1983–1991.
Tang K, Finley Jr RL, Nie D and Honn KV. (2000). *Biochemistry*, **39**, 3185–3191.
Vallejo M, Ron D, Miller CP and Habener JF. (1993). *Proc. Nat. Acad. Sci. USA*, **90**, 4679–4683.
Vinson CR, Hai T and Boyd SM. (1993). *Genes Dev.*, **7**, 1047–1058.
Wadle A, Thiel G, Mischo A, Jung V, Pfreundschuh M and Renner C. (2001). *Oncogene*, **20**, 5920–5929.
Wilcox JN. (1993). *J. Histochem. Cytochem.*, **41**, 1725–1733.
Wilkin F, Suarez-Huerta N, Robaye B, Peetermans J, Libert F, Dumont JE and Maenhaut C. (1997). *Eur. J. Biochem.*, **248**, 660–668.
Yao KS, Clayton M and O'Dwyer PJ. (1995). *J. Nat. Cancer Inst.*, **87**, 117–122.
Yao KS, Xanthoudakis S, Curran T and O'Dwyer PJ. (1994). *Mol. Cell. Biol.*, **14**, 5997–6003.